Single Site Electronic Spectroscopy of Zinc and Magnesium Chlorin in *n*-Octane Matrixes at 7 K

Amarnauth Singh, Wen-Ying Huang, Rachel Egbujor, and Lawrence W. Johnson*

Department of Chemistry, York College of The City University of New York, Jamaica, New York 11451

Received: July 27, 2000; In Final Form: January 17, 2001

The high resolution, single site fluorescence and absorption spectra of zinc and magnesium chlorin in *n*-octane matrixes at 7 K are reported. Both the Q and Soret band regions have been investigated. The vibrational frequencies of the ground and four lowest energy $\pi\pi^*$ singlet excited states were determined from fluorescence and excitation spectra, respectively. The fluorescence and Q_y region spectra are similar, having intense, narrow origin bands followed by relatively weak but orderly vibrational structure. The Q_x regions of these two metal chlorins do not have clear origins and exhibit complex vibrational structure which increases in intensity going to higher energy. In the Soret regions, the individual $\pi\pi^*$ origins are clearly identifiable and some vibrational structure is also observed.

1. Introduction

The electronic spectroscopy of chlorophyll has been and still is an area of vigorous research because of this moietie's role in photosynthesis.[1−5] Because chlorin is the parent compound of chlorophyll, the understanding of its electronic excited states is an important goal. More recently, chlorins have stimulated even more interest because of their possible use as photosensitizers in photodynamic therapy.[6,7]

There have been numerous high-resolution spectroscopic studies[8−15] carried out on free base chlorin (H_2Ch); however, this has not been true for metallochlorins (MCh, Figure 1 inset). There has been some room temperature, solution spectroscopy[16−18] done on the metal complexes (e.g., ZnCh), but no high resolution studies. (In ref 19, there is an indication that some high resolution work was carried out on a Shpolskii matrix containing CuCh at 4.2 K, but only five vibrational bands are mentioned and no spectrum is shown.)

The UV-visible spectroscopy of metallochlorins is generally understood theoretically by the Gouterman four-orbit model. The lowering of the metal porphin symmetry from D_{4h} to C_{2v} destroys the degeneracy of the e_g LUMO and splits the accidentally degenerate HOMO a_{1u} and a_{2u} orbitals. The result is that the strong Q_y transition is followed by a weak Q_x transition. The Soret band components, B_x and B_y, are very intense and are predicted to be very close in energy. Numerous theoretical calculations have been done on metallochlorins in attempt to understand their electronic structure in more detail.[1,20−25]

Two problems in MCh electronic spectroscopy have been locating the Q_x origin and determining the separation of B_x and B_y. Polarization studies on a room-temperature spectrum of magnesium tetraphenylchlorin assigned a weak peak, 700 cm^{-1} above the Q_y origin, as the Q_x 0−0 band.[26] However, on the basis of a magnetic circular dichroism (MCD) study of a room-temperature solution of ZnCh, Keegan et al.[16] made a different assignment of the Q_x origin; they placed it about 1500 cm^{-1} above the Q_y 0−0 band. The Soret band in a room temperature solution spectrum is generally believed to contain two origins in close proximity, but they have not been observed.[1]

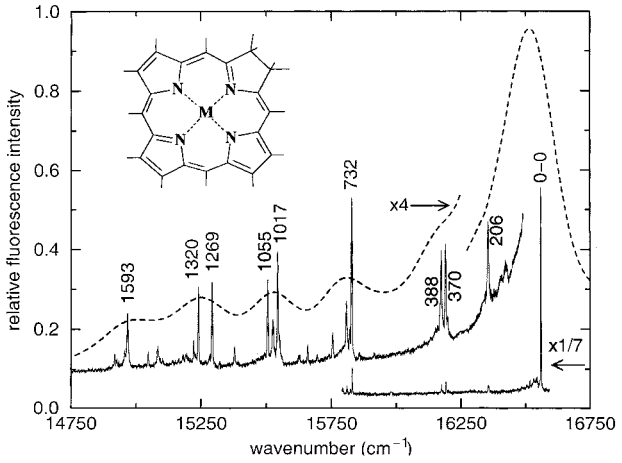

Figure 1. Emission spectra of zinc chlorin in *n*-octane: crystal at 7 K (—); solution at 298 K (− −). The $S_1 \rightarrow S_0$ origin band at 7 K (—) is included. The inset in the figure shows the metallochlorin molecule.

Our intention in this work was to use the resolution afforded by MCh/*n*-octane mixed crystals and Shpolskii matrixes at liquid helium temperatures to examine the details of metallochlorin absorption and emission spectra. We began this study with ZnCh. The initial choice of this metal ion complex came from a number of considerations. First, this ion is believed to lie in the plane of the porphyrin ring,[27] thus giving the molecule approximately C_{2v} symmetry and producing a good substitutional fit into the *n*-octane crystal matrix. Furthermore, porphyrin complexes containing this metal ion have strong fluorescence,[28] which is important for obtaining absorption spectra in the form of excitation spectra. We concluded this study with MgCh, which in relation to photosynthesis, is the most important of the metallochlorins. However, it was more difficult to work with: it has a low fluorescence yield, there is some indication that the magnesium ion is out of the plane of the ring, and it is known to attach axial ligands.[29,30]

* To whom correspondence should be addressed.

10.1021/jp002687f CCC: $20.00 © 2001 American Chemical Society
Published on Web 05/25/2001

In this work, we present the single site fluorescence and excitation spectra of ZnCh and MgCh in *n*-octane matrixes at 7 K. We set out to identify the origins of the first four $\pi\pi^*$ singlet states—Q_y, Q_x, B_x, and B_y—and their associated vibrational structure. Here we also provide a detailed examination of the fluorescence spectra of ZnCh and MgCh.

2. Experimental Section

The metallochlorins were synthesized using a modified version of the procedure developed by Egorova et al.[31] to obtain H_2Ch and MgCh. The zinc ion was inserted into H_2Ch using the technique developed by Adler et al.[32] Dilute solutions of ZnCh and MgCh in purified *n*-octane (*n*-C_8) were prepared; room-temperature electronic absorption and emission spectra were obtained using a Perkins-Elmer (Lambda 19) UV/VIS/NIR spectrometer and a (LS 50B) luminescence spectrometer, respectively. To make MCh/*n*-C_8 mixed crystals, the pure MCh was first put under vacuum ($\sim 10^{-6}$ Torr) overnight, which was done to remove any remaining solvent molecules; then the dilute solutions ($\sim 10^{-6}$ M) were degassed, sealed in Pyrex tubes, and then slowly lowered ($\sim$24 h) into liquid nitrogen. The resulting single crystals were cut under liquid nitrogen and cooled to 7 K using an Oxford Instruments CF1204 cryostat.

High-resolution absorption spectra of each complex were obtained in the form of excitation spectra at liquid helium temperature. The initial scans were made with a Jobin-Yvon THR1500 monochromator with its optical axis perpendicular to the laser excitation beam, its wavelength set to zero so as to monitor the total emission, and using two 630 nm cutoff filters inserted in front of the entrance slit; the origin area of the $S_1 \leftarrow S_0$ excitation was scanned with a Lambda Physik 2001 dye laser (bandwidth 0.2 cm^{-1}) pumped with a Lambda Physik Lextra 50 (XeCl) excimer laser. To obtain single site spectra, the molecule's emission and the laser's intensity were monitored using two EMI 9203QA phototubes in cooled housings and a Stanford Instruments SR400 photoncounter. The monochromator's wavelength was then set to a Q_y 0−0 band, and the vibronic and higher energy excitation spectra were scanned with the dye laser; these excitation spectra were corrected by software for the wavelength dependence of the laser's intensity. The single-site excitation spectra of the origin regions were obtained by setting the monochromator at a strong vibrational emission band and then by scanning the dye laser over the origin. The dyes used to cover the excitation spectra were Exciton's C540A, C500, C480, C440, and QUI and Lambda Chrome's LC3990.

High-resolution emission spectra were obtained at 7 K for the two complexes. The Lambda Physik 2001 dye laser was set at the $S_1 \leftarrow S_0$ 0−0 band, and the emission spectrum was scanned using the Jobin-Yvon 1500 monochromator in conjunction with a Stanford Instruments SR510 lock-in amplifier. The single site emission origins were obtained by setting the laser's wavelength on a strong vibrational band in the excitation spectrum and then scanning the monochromator over the emission spectrum. The emission spectrum reported for MgCh/*n*-C_8 at 7 K was obtained using a Shpolskii matrix because the crystal gave the same spectral features but a much weaker fluorescence intensity.

3. Results and Discussion

3.1. Fluorescence. Figures 1 and 2 show the fluorescence spectra of ZnCh and MgCh, respectively. The dotted lines are the low resolution emission spectra made with room temperature *n*-octane solutions. The solid line spectra were made with the metallochlorins in *n*-octane matrixes at 7 K. The origins of the ZnCh and MgCh emissions are at 16 548 cm^{-1} and 16 498 cm^{-1}, respectively. The vibrational peak positions for the two 7 K spectra are listed in Tables 1 and 2. These tables include each peak's distance from the origin in cm^{-1} and its relative intensity to the origin; each origin was arbitrarily assigned an intensity value of 1000. We have also included tentative assignments of each vibrational peak and the corresponding ground-state vibration determined from infrared and Raman spectroscopy on CuCh.[19]

The vibrational patterns of the two metallochlorins are very similar. (The single site spectrum of MgCh exhibits small amounts of contamination by other nearby sites which could not be totally excluded; however, in each case, these bands are at least an order of magnitude less intense than those belonging to the site under investigation, so any contributions to the spectrum are barely above the noise.) The major differences in

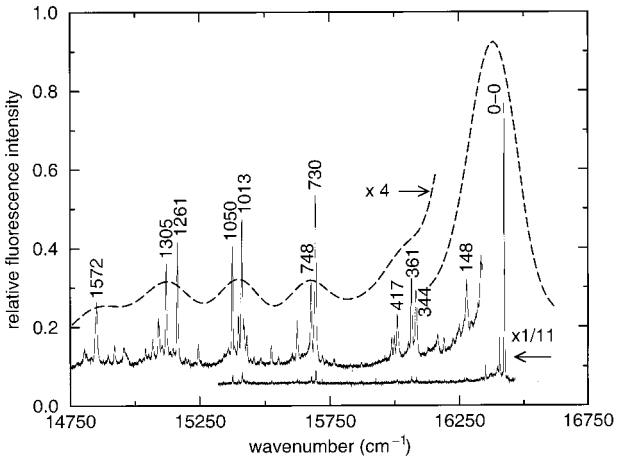

Figure 2. Emission spectra of magnesium chlorin in *n*-octane: Shpolskii matrix at 7 K (—); solution at 298 K (– –). The $S_1 \rightarrow S_0$ origin band at 7 K (—) is included.

TABLE 1: Vibrational Frequencies Obtained from the Single Site Emission Spectrum of Zinc Chlorin in an *n*-Octane Crystal at 7 K

ν_{gd} (cm^{-1})[a]	I[b]	assignment[c]	CuCh[d]
0	1000	0−0 ($S_1 \rightarrow S_0$)	
25	45	phonon	
206	72	F	202
370	86	F	366
388	80	F	385
732	143	F	730
740	27	F or (370 × 2)	744
753	53	F or (370+388)−5	766
805	37	F	804
901	20	F	900
1017	100	F	1008
1035	38	F	1035
1055	75	F	1056
1183	20	F	1175
1269	80	F	1267
1320	78	F	1325 or 1316
1339	24		
1476	20	F or (206+1269)+1	1475
1514	19	F	1515
1593	53	F	1597
1642	14	F	1649

[a] Distance of the spectral feature from the $S_1 \rightarrow S_0$ origin (16 548 cm^{-1}). [b] The $S_1 \rightarrow S_0$ origin's intensity I was independently assigned a value of 1000; all subsequent peaks were compared to it. [c] F signifies a fundamental vibration. [d] Ground-state vibrations of CuCh from infrared and Raman spectroscopy (ref 19).

TABLE 2: Vibrational Frequencies Obtained from the Single Site Emission Spectrum of Magnesium Chlorin in an *n*-Octane Shpolskii Matrix at 7 K

ν_{gd} (cm^{-1})[a]	I[b]	assignment[c]	CuCh[d]
0	1000	0−0 ($S_1 \rightarrow S_0$)	
28	25	phonon	
148	29	F	
344	27	F	366
361	32	F	385
417	19	F	
425	9	F	
437	9	F	
730	58	F	730
748	29	F	744
800	17	F	804
901	9	F	900
995	10	F	998
1005	12		
1013	46	F	1008
1026	19	F	1035
1050	40	F	1056
1181	9	F	1175
1261	37	F	1267
1305	29	F	1302
1336	18	F	1333
1356	13	F	1355
1386	8	F or (361+1026)−1	1384
1503	9	F or (148+1356)−1	1515
1572	21	F	1597
1618	8	F or (361+1261)−4	1647

[a] Distance of the spectral feature from the $S_1 \rightarrow S_0$ origin (16 498 cm^{-1}). [b] The $S_1 \rightarrow S_0$ origin's intensity I was independently assigned a value of 1000; all subsequent peaks were compared to it. [c] F signifies a fundamental vibration. [d] Ground-state vibrations of CuCh from infrared and Raman spectroscopy (ref 19).

the spectra are in the MgCh emission (Figure 2) at 148 and 417 cm^{-1} from the origin.

At 417 cm^{-1}, there is a group of three peaks which have no counterpart in the ZnCh emission spectrum. This is not one of the vibrational energies listed in the infrared or resonance Raman spectra of CuCh.[19] (However, in the Raman spectrum shown in ref 19, there is a very weak peak at about 410 cm^{-1}.) Some supporting evidence that these three peaks in the emission spectrum belong to MgCh comes from the fact that a peak at 417 cm^{-1} is also seen in the excitation spectrum; furthermore, when we set the monochromator's wavelength to each of these peaks and scanned the laser, we obtained the same MgCh single site excitation spectrum (0−0 at 16 498 cm^{-1}). Because these peaks are only seen in the MgCh spectrum, they presumably arise as a result of some novel way in which Mg^{2+} fits into the ring's cavity or the effect of an axial ligand. In a resonance Raman study of copper (II) tetraphenylchlorin,[33] a peak was observed at 419 cm^{-1}, which on the basis of a normal coordinate analysis was partially attributed to an in-plane deformation involving the metal, the reduced pyrrole ring, and the pyrrole ring opposite it.

In the ZnCh fluorescence spectrum, the first major vibrational peak is at 206 cm^{-1}. In the MgCh spectrum, the corresponding peak is at 148 cm^{-1}. The ∼200 cm^{-1} bands are usually assigned to a metal−nitrogen vibration.[34] Consequently, this ∼50 cm^{-1} reduction in the lowest energy vibration of MgCh maybe another indication that the Mg ion has an axial ligand attached to it.[35]

3.2. Absorption. The absorption spectra of ZnCh and MgCh have been obtained in the form of excitation spectra. The full spectra of the Q through B regions (16 000−26 000 cm^{-1}) for these metallochlorins are shown in Figures 3 and 4; the peak positions are listed in Tables 3 and 4, respectively. In each spectrum, the $S_1 \leftarrow S_0$ origin has been arbitrarily assigned an intensity value of 1000, and all other peak intensities in the spectrum are based on that assumption; each table also gives the peak position relative to the $S_1 \leftarrow S_0$ origin, an estimated assignment, and the corresponding CuCh ground-state vibration.[19] The dotted line in each figure is the room-temperature solution excitation spectrum, and the solid line is the excitation spectrum that was made at 7 K.

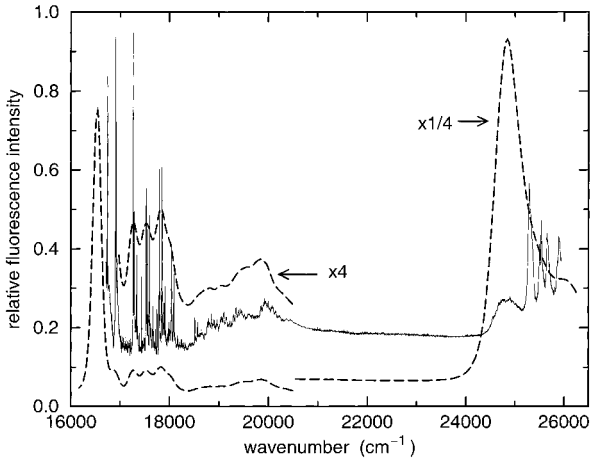

Figure 3. Excitation spectra of zinc chlorin in *n*-octane: crystal at 7 K (—); solution at 298 K (−−). Both the Q and Soret regions are shown.

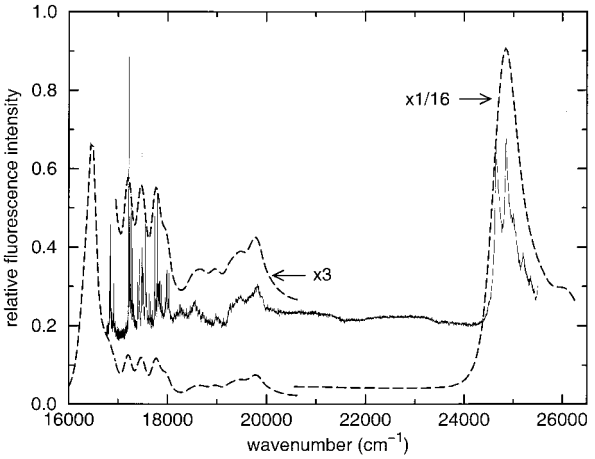

Figure 4. Excitation spectra of magnesium chlorin in *n*-octane: crystal at 7 K (—); solution at 298 K (−−). Both the Q and Soret regions are shown.

An expanded view of the Q_y regions (16 500−18 250 cm^{-1}) of ZnCh and MgCh are shown in Figures 5 and 6, respectively. The Q_y origin positions and full widths at half-maximum (fwhm) at 7 K are as follows: ZnCh, 16 548 cm^{-1} and 1.0 cm^{-1}; MgCh, 16 498 cm^{-1} and 1.2 cm^{-1}. The Q_y region of ZnCh is very similar to the mirror image of its fluorescence spectrum; this indicates that the ground and first excited states have similar geometries. The Q_y region of MgCh, although generally the same as that of ZnCh, exhibits some differences. First, the MgCh $S_1 \leftarrow S_0$ origin is red shifted by 50 cm^{-1} with respect to ZnCh. Second, there is a vibrational peak at 417 cm^{-1} which is not in the excitation spectrum of the ZnCh complex; this peak is present in the MgCh fluorescence spectrum, as discussed earlier. Third, the low energy vibrational peak, which is at about 197 cm^{-1} in the ZnCh spectrum and at 148 cm^{-1} in the MgCh fluorescence spectrum, is missing. This is reminiscent, but opposite, of what was observed for magnesium porphin (MgP)

TABLE 3: Vibrational Frequencies Obtained from the Single Site Excitation Spectrum of Zinc Chlorin in an *n*-Octane Crystal at 7 K

ν_{exc} (cm^{-1})[a]	I[b]	assignment[c]	CuCh[d]	ν_{exc} (cm^{-1})[a]	I[b]	assignment[c]	CuCh[d]
0	1000	0−0 (S_1←S_0)		2297	17	(991+1301)+5	
197	168	F	202	2326	13	(1125+1202)−1	
362	235	F	366	2335	8	(1125+1209)+1	
377	170	F	385	2353	12	(1054+1301)−2	
719	228	F	730	2384	9	(890+1493)+1	
740	90	F	740	2410	13	(1202+1209)−1	
784	25	F	804	2432	9	(1125+1306)+1	
794	66	F	819	2481	9	(991+1493)−3	
890	59	F	900	2499	13	(1250 × 2)−1	
976	105	F	975	2514	11	(1020+1493)+1	
991	109	F	998	2535	12	(991+1548)−4	
1020	85	F	1035	2542	15	(1054+1493)−5	
1054	102	F	1056	2553	17	(1054+1498)+1	
1119	24	(377+740)+2		2579	8	(1250+1335)−6	
1125	27	F	1152	2594	12	(362+976+1250)+6	
1202	30	F	1215	2610	12	(1306 × 2)−2	
1209	25	F	1222	2639	6	(1306+1335)−2	
1250	137	F	1265	2654	6	(377+076+1306)−5	
1301	70	F	1302	2668	9	(1306+1365)−3	
1306	132	F	1314	2695	8	(1202+1493)	
1335	14	F or (362+976)−3	1333	2711	7	(1209+1498)+4	
1348	20	(377+976)−5		2745	14	(1250+1493)+2	
1354	22	(362+991)+1		2764	10	(1209+1548)+7	
1365	40	F or (377+991)−3	1365	2797	19	(1306+1493)−2	
1493	65	F	1485	2853	17	(1306+1548)−1	
1498	50	F	1515	2881	18	(890+976+1020)−5	
1503	35	(197+1306)		2910	17	(377+991+1548)−6	
1538	30	F	1536	2967	14	(991 × 3)−6	
1548	50	F	1550	3062	14	(1020 × 3)+2	
1562	10	(197+1365)		3298	15	(890+1202 × 2)+4	
1613	14	(362+1250)+1		3307	15	(1054+1125 × 2)+3	
1629	8	(377+1250)+2		3374	19	(1125 × 3)−1	
1667	10	(362+1306)−1		3447	17	(1125 × 2+1202)−5	
1693	11	(387+1306)		3507	12	(1125 × 2+1250)+7	
1709	14	(719+991)−1		3525	14	(1020 × 2+1493)−8	
1737	11	(719+1020)−2		3545	13	(377 × 2+740 × 2)+5	
1772	12	(719+1054)−1		3600	9	(1202 × 3)−6	
1777	11	(890 × 2)−3		3674	6	(719+740 × 4)−5	
1789	12	(794+991)+4		3745	8	(1125 × 2+1493)+2	
1968*	20	(719+1250)−1		3817	8	(719+1548 × 2)+2	
1988	6	(740+1250)−2		3891	8	(1202 × 2+1493)−6	
2023*	14	(719+1306)−4		8243	100	0−0′ (S_3←S_0)	
2068	5	(377+719+976)−4		8749	400	0−0″ (S_4←S_0)[e]	
2225	13	(1020+1202)+3		8953 (204″)[e]	246	F	204
2242	16	(991+1250)+1		8989 (240″)[e]	307	F	248
2255	11	(1054+1202)−1		9105 (356″)[e]	276	F	366
2269	10	(719+1548)+2		9343 (594″)[e]	266	(240″+356″)−2[e]	
2281	8	(976+1306)−1					

[a] Distance of the spectral feature from the $S_1 \leftarrow S_0$ origin (16 548 cm^{-1}). [b] The $S_1 \leftarrow S_0$ origin's intensity I was independently assigned a value of 1000; all subsequent peaks were compared to it. [c] F signifies a fundamental vibration. [d] Ground-state vibrations of CuCh from infrared and Raman spectroscopy (ref 19). [e] The double prime (″) indicates the distance of the spectral feature from the $S_4 \leftarrow S_0$ origin (25 297 cm^{-1}).

complexed with ethanol in an *n*-octane crystal at 4.2 K;[36] in this case, the absorption spectrum shows a weak peak 198 cm^{-1} above the origin, but the fluorescence spectrum shows no peak in that region. For ZnP complexed and uncomplexed with ethanol, this low energy vibrational band is present in the absorption and fluorescence spectra.[36] Because magnesium forms axial complexes much more tenaciously than zinc, the present/absent character of this peak may be indicative of changes in the metal−ligand complex between the ground and excited state.

Expanded views of the ZnCh and MgCh Q_x regions (18 000−20 250 cm^{-1}) are shown in Figures 7 and 8, respectively. There is no obvious origin band in these spectra; previous attempts to assign its position have left it uncertain.[16,25] For example, Keegan et al.[16] carried out an MCD experiment on ZnCh in a room-temperature benzene solution; they "tenuously" assigned a negative MCD band at 555 nm as corresponding to the Q_x origin. After compensating for a solvent shift of about 3 nm to the blue in going from benzene to *n*-octane, this put the Q_x 0−0 at about 18 100 cm^{-1} in our spectrum. This corresponds to the last major feature in Figure 5, 1548 cm^{-1} from the Q_y origin. An inspection of ZnCh fluorescence in Figure 1 shows a similar peak, 1593 cm^{-1} from the Q_y origin; this implies that the 555 nm MCD signal is due to a Q_y vibrational band.

Another possibility for the Q_x origin in this MCD spectrum is the negative band, a shoulder, at 546 nm. Correcting this wavelength for the change in solvent and assuming that the peak which produced the shoulder is a little more to the blue gives it a position of about 18 500 cm^{-1} in our spectrum. We believe that this is the correct region for the ZnCh Q_x origin.

At 18 517 and 18 571 cm^{-1}, we encounter a pair of prominent sharp peaks in the ZnCh spectrum. They are identified with

TABLE 4: Vibrational Frequencies Obtained from the Single Site Excitation Spectrum of Magnesium Chlorin in an *n*-Octane Crystal at 7 K

ν_{exc} (cm^{-1})[a]	I[b]	assignment[c]	CuCh[d]	ν_{exc} (cm^{-1})[a]	I[b]	assignment[c]	CuCh[d]
0	1000	0−0 (S_1←S_0)		1578	62	(328+1249)+1	
25	120	phonon		1606	56	F or (357+1249)	1607
328	116	F		1620	54	(328+1293)−1	
338	200	F		1639	66	(350+1293)−4	
350	276	F		1659	60	(338 × 2+978)+5	
354	197	F		1682	73	(338+1345)−1	
357	280	F	366	1702	73	(357+1345)	
417	135	F		1744	85	(745+1000)−1	
706	110	(350+357)−1		1772	87	(338+719 × 2)−4	
719	673	F	730	1798	77	(338+719+745)−4	
736	295	F	744	1831	73	(350+736+745)	
745	179	F		1860	68	(927 × 2)+6	
762	123	F	766	1884	77	(357+736+792)−1	
770	348	F	804	1922	65	(357+792+770)+3	
792	215	F	819	1960	83	(719+1242)−1	
897	146	F	892	1987	79	(745+1242)	
927	229	F		2062	96	(770+1293)−1	
978	448	F	975	2089	82	(745+1345)−1	
985	218	F		2106	81	(762+1345)−1	
989	218	F	992	2142	71	(770+1371)+1	
1000	171	F	1003	2156	75	(719 × 3)−1	
1016	160	F	1032	2198	62	(1000+1198)	
1046	216	F or (328+719)−1	1050	2218	62	(978+1242)−2	
1053	303	F or (338+719)−4	1067	2249	59	(1000+1249)	
1127	113	(357+770)		2343	50	(1000+1345)−2	
1158	93	F or (417+745)−4	1152	2367	51	(1000+1371)−4	
1198	69	F	1175	2402	50	(1198 × 2)+6	
1242	311	F	1222	2475	64	(338+897+1242)−2	
1249	265	F	1265	2504	61	(1249 × 2)+6	
1267	96	(338+927)+2		2633	40	(1293+1345)−5	
1293	361	F	1302	2776	70	(927 × 3)−5	
1318	135	F or (338+978)+2	1314	2814	69	(897 × 2+1016)+4	
1345	230	F	1351	2881	74	(897+989 × 2)+6	
1371	135	F	1374	3222	71	(927 × 2+1371)−3	
1456	100	F or (719+736)+1	1465	3320	86	(978 × 2+1371)−7	
1478	160	(736+745)−3		8152	1338	0−0′ (S_3←S_0)[e]	
1490	164	(719+770)+1		8356	1352	0−0″ (S_4←S_0)[f]	
1530	167	F or (736+792)+2	1536	8506 (354′)[e]	822	366	
1553	74	F or (762+792)−1	1550	8699 (343″)[f]	545	366	

[a] Distance of the spectral feature from the $S_1 \leftarrow S_0$ origin (16 498 cm^{-1}). [b] The $S_1 \leftarrow S_0$ origin's intensity I was independently assigned a value of 1000; all subsequent peaks were compared to it. [c] F signifies a fundamental vibration. [d] Ground-state vibrations of CuCh from infrared and Raman spectroscopy (ref 19). [e] The single prime (′) indicates the distance of the spectral feature from the $S_3 \leftarrow S_0$ origin (24 650 cm^{-1}). [f] The double prime (″) indicates the distance of the spectral feature from the $S_4 \leftarrow S_0$ origin (24 854 cm^{-1}).

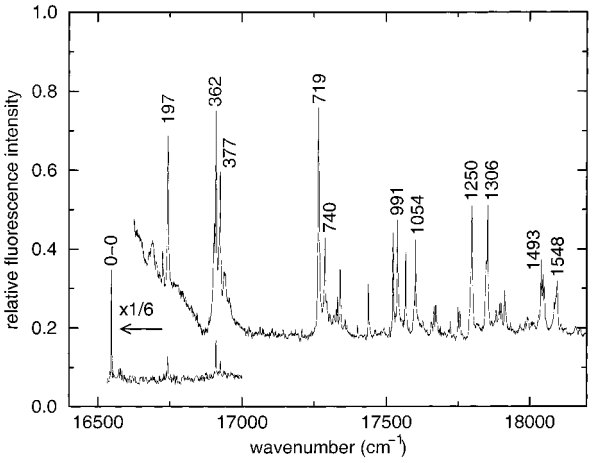

Figure 5. Single site excitation spectrum of zinc chlorin in an *n*-octane crystal at 7 K. Only the Q_y region is shown; the $S_1 \leftarrow S_0$ origin band is included.

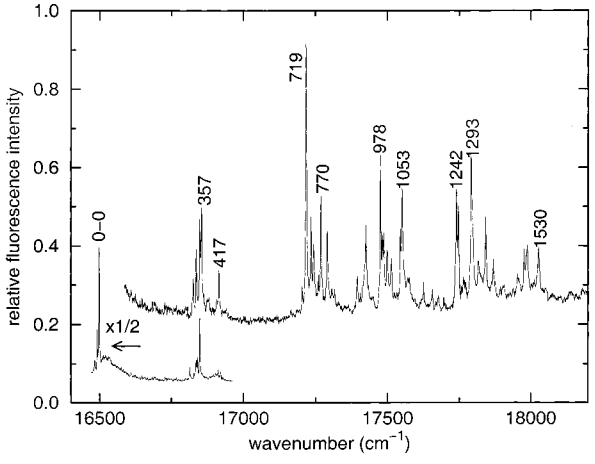

Figure 6. Single site excitation spectrum of magnesium chlorin in an *n*-octane crystal at 7 K. Only the Q_y region is shown; the S_1←S_0 origin band is included.

stars (*) in Figure 7 and Table 3; they are respectively 1968 and 2023 cm^{-1} away from the Q_y origin. These starred pairs then appear to form the basis of the subsequent, complex fine structure which is found in this part of the spectrum. This is illustrated in Figure 7; in this figure, the origin region has been shifted by several vibrational intervals (a−g) to show how it

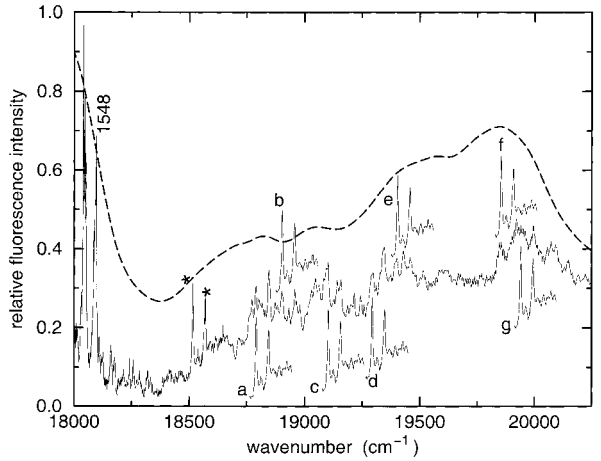

Figure 7. Excitation spectra of zinc chlorin in *n*-octane: crystal at 7 K (—); solution at 298 K (– –). Only the Q_x region is shown. The starred pair of peaks has been shifted by a, 275 cm^{-1}; b, 387 cm^{-1}; c, 587 cm^{-1}; d, 778 cm^{-1}; e, 888 cm^{-1}; f, 1339 cm^{-1}; and g, 1424 cm^{-1}. The assumed Q_x origin region is centered at 18 539 cm^{-1} (- - -).

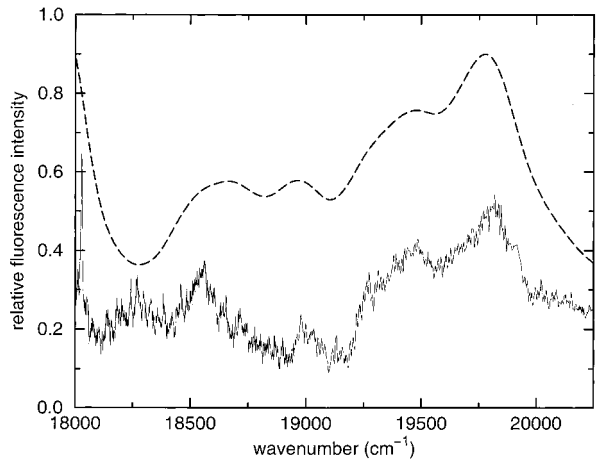

Figure 8. Excitation spectra of magnesium chlorin in *n*-octane: crystal at 7 K (—); solution at 298 K (– –). Only the Q_x region is shown.

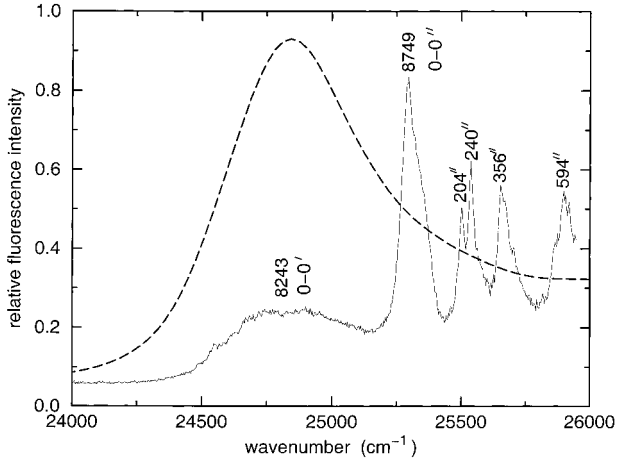

Figure 9. Excitation spectra of zinc chlorin in *n*-octane: crystal at 7 K (—); solution at 298 K (– –). Only the Soret region is shown. The double prime (″) indicates the distance of the spectral feature from the $S_4 \leftarrow S_0$ origin (25 297 cm^{-1}).

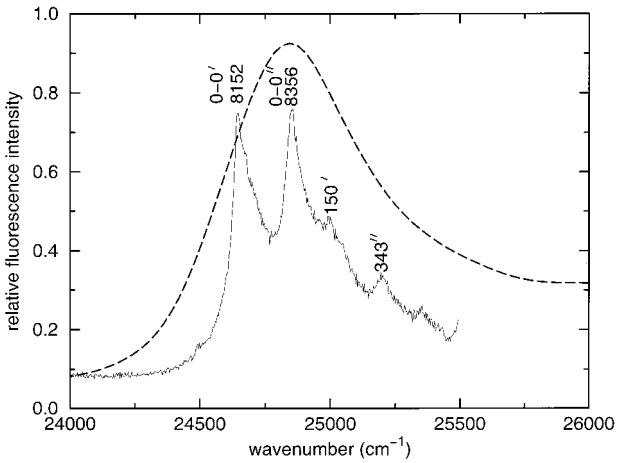

Figure 10. Excitation spectra of magnesium chlorin in *n*-octane: crystal at 7 K (—); solution at 298 K (– –). Only the Soret region is shown. The single prime (′) indicates the distance of the spectral feature from the $S_3 \leftarrow S_0$ origin (24 650 cm^{-1}). The double prime (″) indicates the distance of the spectral feature from the $S_4 \leftarrow S_0$ origin (24 854 cm^{-1}).

generates the Q_x spectrum. Also, the bandwidth (fwhm) of the fine structure steadily increases across this region, starting at about 5 cm^{-1} and reaching about 25 cm^{-1} at the end. The first starred peak (18 517 cm^{-1}) has a fwhm of 5 cm^{-1}; by position d (19 285 cm^{-1}) of the starred peaks, the fwhm has reached about 18 cm^{-1}, and by position f (19 851 cm^{-1}), it is up to about 24 cm^{-1}. This large increase in fwhm of the fine structure bands is consistent with the assumption that this is where the Q_y state is penetrating the Q_x state.[42] (This is different from the Q_y region, where the fwhm of the spectral features goes from 1 to 5 cm^{-1}.)

This type of complex, often called "tangled", spectral pattern has previously been observed in large organic molecules,[37] including simple porphyrins,[38,39] in the area of the second electronic transition and is due to the resonant coupling between the higher energy excited state and the background manifold of vibrations from the lower excited state.[40,41] The ZnCh Q_x origin region (~18 490−18 590 cm^{-1}; Figure 7, dashed line) is thought to have a fwhm of about 70 cm^{-1}; this represents the magnitude of the vibronic interaction between the two states.

In previous examples of resonant coupling, the spectra were highly structured, but maintained the overall shape common to many $\pi\pi^*$ transitions where there is only a minor change in geometry; that is, there is an intense origin region followed by substantially less intense spectral features due to excited-state vibrations. However, these metallochlorins (ZnCh and MgCh) exhibit a low intensity origin region, followed by an absorption which increases in intensity; this suggests that the transition to this excited state may be accompanied by a change in molecular geometry. This overall band shape arises because the potential energy curve of the excited state is shifted with respect to that of the ground state; consequently, the origin band may have little or no oscillator strength because of a small Franck−Condon factor, whereas the transitions to excited-state vibrational levels obtain larger relative intensities because of enhanced overlap of the wave functions.

Figure 8 shows the Q_x region of MgCh. The contour is similar to that of ZnCh, but the fine structure is just above the noise level, so no detailed analysis was possible.

The Soret regions of ZnCh and MgCh are shown in Figures 9 and 10, respectively. In Figure 9, the broad band at about 24 790 cm^{-1} was assigned as the B_x origin of ZnCh. The relatively strong and sharp peak at 25 297 cm^{-1} was assigned as the B_y origin. This 0−0 band is followed by a series of four vibrational bands; they all correlate well with symmetric (A) vibrations determined from CuCh.[19] The Soret band measured

at 7 K is dramatically different than the one measured at 298 K. We were initially concerned that this change might be an artifact. To verify our results, we excited the molecule at various points in this region (e.g., 24 790 and 25 297 cm^{-1}) and obtained the normal fluorescence spectrum from each position. There has been some speculation that the Q_y and B states have different geometries.[43] However, we cannot draw any conclusions about this from our data. The striking bandwidth difference between the B_x (fwhm, ~570 cm^{-1}) and the B_y (fwhm, ~110 cm^{-1}) origins probably arises from their distinct lifetimes and methods of relaxation. The broad B_x presumably has a short lifetime. Its low intensity in the 7 K excitation spectrum indicates that it is not primarily relaxing via Q_y fluorescence. Because we did not observe emission from the B_x state, we concluded that its large fwhm and weak intensity is the result of an efficient dark pathway. The B_y band, on the other hand, should have a relatively long lifetime and relax via a fluorescent route; consequently, it is relatively narrow and intense in the excitation spectrum.

The MgCh B_x and B_y bands (Figure 10) at 24 650 and 24 854 cm^{-1}, respectively, are both strong and relatively narrow (~140 cm^{-1}), indicating that they have relatively long lifetimes and relax via an efficient Q_y emitting pathway. Following each of these origins, there appears to be at least one weak vibrational band. As in the case of ZnCh, the vibration seems to corresponds to a symmetric mode.[19]

The B_x-B_y splittings measured here—ZnCh, 506 cm^{-1} and MgCh, 204 cm^{-1}—confirm theoretical predictions that B_x and B_y are essentially degenerate.[1]

4. Conclusion

We have accurately identified the 0−0 positions of Q_y, B_x, and B_y bands for these two metallochlorins, ZnCh and MgCh. For both molecules, a Q_x origin band is not evident; however, it seems to be undergoing a resonant coupling with the higher vibrational levels of the Q_y band. Furthermore, the increasing intensity of the band in going from its apparent origin toward higher energy is suggestive of a change in molecular geometry associated with this state. In the Soret region, we can clearly identify the origins of the two nearly degenerate transitions (B_x and B_y) and some associated vibrational activity.

Acknowledgment. We would like to thank Professor Martin Gouterman for his insightful and helpful comments on the manuscript. We also thank Martin Sadilek, also of the University of Washington, for his assistance with the mass spectrometry of the samples. This investigation was supported by the National Institutes of Health (GM08153).

References and Notes

(1) Gouterman, M. In *The Porphyrins*; Dolphin, D., Ed.; Academic Press: New York, 1978; Vol. III, p 1.
(2) Weiss, C. In *The Porphyrins*; Dolphin, D., Ed.; Academic Press: New York, 1978; Vol. III, p 211.
(3) Hall, D. D.; Rao, K. K. *Photosynthesis*, 5th ed.; Cambridge University Press: Cambridge, U.K., 1995.
(4) Kadish, K. M., Smith, K. M., Guilard, R., Eds.; *The Porphyrin Handbook*; Academic Press: New York, 2000.
(5) Parusel, A. B. J.; Grimme, S. *J. Phys. Chem. B* **2000**, *104*, 5395.
(6) Pandoy, R. K.; Zheng, G. Porphyrins as Photosensitizers in Photodynamic Therapy. In *The Porphyrin Handbook*; Kadish, K. M., Smith, K. M., Guilard, R., Eds; Academic Press: New York, 2000; Vol. 6.
(7) Blant, S. A.; Ballini, J. P.; van den Bergh, H.; Fontolliet, C.; Wagnieres, G.; Monnier, P. *Photochem. Photobiol.* **2000**, *71*, 33.
(8) Völker, S.; Macfarlane, R. M. *J. Chem. Phys.* **1980**, *73*, 4476.
(9) Dicker, A. I. M.; Dobkowski, J.; Noort, M.; Völker, S.; van der Waals, J. H. *Chem. Phys. Lett.* **1982**, *88*, 135.
(10) Dicker, A. I. M.; Noort, M.; Thijssen, H. P. H.; Völker, S.; van der Waals, J. H. *Chem. Phys. Lett.* **1978**, *78*, 212.
(11) Dicker, A. I. M.; Johnson, L. W.; Noort, M.; van der Waals, J. H. *Chem. Phys. Lett.* **1983**, *94*, 14.
(12) Burkhalter, F. A.; Suter, G. W.; Wild, U. P. *Chem. Phys. Lett.* **1983**, *94*, 483.
(13) Solovyov, K. N.; Sevchenko, A. N.; Mashenkov, V. A.; Shkirman, S. F. *Sov. Phys. Dokl.* **1966**, *10*, 778.
(14) Huang, W.-Y.; Rebane, A.; Wild, U. P.; Johnson, L. W. *J. Lumin.* **1997**, *71*, 237.
(15) Huang, W.-Y.; VanRiper, E.; Johnson, L. W. *Spectrochim. Acta Part A* **1996**, *52*, 761.
(16) Keegan, J. D.; Stolzenberg, A. M.; Lu, Y.-C.; Linder, R. E.; Barth, G.; Moscowitz, A.; Bunnenberg, E.; Djerassi, C. *J. Am. Chem. Soc.* **1982**, *104*, 4317.
(17) Eisner, U.; Linstead, R. P. *J. Chem. Soc.* **1955**, 3749.
(18) Blackwood, M. E.; Kumble, R.; Spiro, T. G. *J. Phys. Chem.* **1996**, *100*, 18037.
(19) Solovyov, K. N.; Gladkov, L. L.; Gradyushko, A. T.; Ksenofontova, N. U.; Shulga, A. M.; Starukhin, A. S. *J. Mol. Struct.* **1978**, *45*, 267.
(20) Weiss, C., Jr. *J. Mol. Spectrosc.* **1972**, *44*. 37.
(21) Petke, J. D.; Maggiora, G. M.; Shipman, L. L.; Christoffersen, R. E. *J. Mol. Spectrosc.* **1978**, *73*, 311.
(22) Hasegawa, J.; Ozeki, Y.; Ohkawa, K.; Hada, M.; Nakatsuj, H. *J. Phys. Chem. B* **1998**, *102*, 1326.
(23) Spangler, D.; Maggiora, G. M.; Shipman, L. L.; Christoffersen, R. E. *J. Am. Chem. Soc.* **1977**, *99*, 7478.
(24) Parusel, A. B.; Ghosh, A. *J. Phys. Chem. A* **2000**, *104*, 2504.
(25) Gosh, A. In *The Porphyrin Handbook*; Kadish, K. M., Smith, K. M., Guilard, R., Eds.; Academic Press: New York, 2000; Vol. 7.
(26) Sevchenko, A. N.; Solov'ev, K. N.; Mashenkov, V. A.; Shkirman, S. F.; Losev, A. P. *Sov. Phys. Dokl.* **1968**, *12*, 787.
(27) Buchler, J. W. Static Coordination of Metalloporphyrins. In *Porphyrins and Metalloporphyrins*; Smith, K. M., Ed.; Elsevier Scientific Publishing Co.: Amsterdam, The Netherlands, 1975.
(28) Becker, R. S.; Allison, J. B. *J. Phys. Chem.* **1963**, *67*, 2669.
(29) Dicker, A. I. M.; Johnson, L. W.; Völker, S.; van der Waals, J. H. *Chem. Phys. Lett.* **1983**, *100*, 46.
(30) Platenkamp, R. J.; Noort, M. *Mol. Phys.* **1982**, *45*, 97.
(31) Egorova, G. D.; Soloveu, K. N.; Shulga, A. M. *Zh. Obsach. Khim.* **1967**, *37*, 357.
(32) Adler, A. D.; Longo, F. R.; Kampos, F.; Kim, J. J. *Inorg. Nucl. Chem.* **1970**, *32*, 2443.
(33) Donohue, R. J.; Atamian, M.; Bocian, B. F. *J. Phys. Chem.* **1989**, *93*, 2244.
(34) Burger, H. Vibrational Spectroscopy of Porphyrins and Metalloporphyrins. In *Porphyrins and Metalloporphyrins*; Smith, K. M., Ed.; Elsevier Scientific Publishing Co.: Amsterdam, The Netherlands, 1975.
(35) Ozaki, Y.; Iriyama, K.; Ogoshi, H.; Ochiai, T.; Kitagawa, T. J. *Phys. Chem.* **1986**, *90*, 6113.
(36) Jansen, G.; Noort, M. *Spectrochim. Acta* **1976**, *32A*, 747.
(37) Wessel, J.; McClure, D. S. *Mol. Cryst. Liq. Cryst.* **1980**, *58*, 121.
(38) Huang, W.-Y.; Johnson, L. W. *J. Chem. Phys.* **1998**, *108*, 4349.
(39) Huang, W.-Y.; VanRiper, E.; Johnson, L. W. *Spectrochim. Acta A* **1996**, *53*, 589.
(40) Langhoff, C. A.; Robinson, G. W. *Chem. Phys.* **1974**, *6*, 34.
(41) Freed, K. F. Energy Dependence of Electronic Relaxation Processes in Polyatomic Molecules. In *Topics in Applied Physics*; Radiationless Processes in Molecules and Condensed Phases; Fong, K. F., Ed.; Springer-Verlag: New York, 1976; Vol. 15.
(42) Hochstrasser, R. M. *Acc. Chem. Res.* **1968**, *1*, 266.
(43) Prendergust, K.; Spiro, T. G. *J. Phys. Chem.* **1991**, *95*, 1555.